ChemPubSoc Europe

DOI: 10.1002/chem.201400082

CHEMISTRY
A European Journal
Full Paper

Helical Structures

Synthesis and Structures of *N*-Alkyl-1,13-dimethoxychromeno-[2,3,4-*kl*]acridinium Salts: The Missing Azaoxa[4]helicenium

Thomas Just Sørensen, Anders Ø. Madsen, and Bo W. Laursen*[a]

Abstract: Helical structures are interesting due to their inherent chirality. Helicenium ions are triarylmethylium structures twisted into configurationally stable helicenes through the introduction of two heteroatom bridges between the three aryl substituents. Of the configurationally stable [4]helicenium ions, derivatives with sulfur, oxygen and nitrogen bridges have already been synthesised. However, one [4]helicenium ion has proven elusive, until now. We present herein the first synthesis of the 1,13-dimethoxychromeno-[2,3,4-*kl*]acridinium ($DMCA^+$) [4]helicenium ion. A series of six differently *N*-substituted $DMCA^+$ ions as their hexafluorophosphate salts are reported. Their cation stability was evaluated and it was found that $DMCA^+$ is ideally suited as a phase-transfer catalyst with a pK_{R+} of 13.0. The selectivity of nucleophilic addition to the central carbon atom of $DMCA^+$ has been demonstrated with diastereotopic ratios of up to 1:10. The single-crystal structures of several of the $DMCA^+$ salts were determined, and structural differences between *N*-aryl- and *N*-alkyl-substituted cations were observed. The results of a comparative study of the photophysics of the [4]helicenium ions are presented. $DMCA^+$ is found to be a potent red-emitting dye with a fluorescence quantum yield of 20% in apolar solvents and a fluorescence lifetime of 12 ns. [4]Helicenium ions, including $DMCA^+$, all suffer from solvent-induced quenching, which reduces the fluorescence quantum yields significantly ($\phi_{fl} < 5\%$) in polar solvents. A difference in photophysical properties is observed between *N*-aryl- and *N*-alkyl-substituted $DMCA^+$, which has tentatively been attributed to a difference in molecular conformation.

Introduction

The synthesis of carbo- and heterohelicenes has proven a challenge,[1] which has spurred on considerable efforts towards the synthesis and resolution of various types of helical structures.[2] [4]Helicene is the smallest helicene (Figure 1), with four condensed aromatic rings. The helical pitch of [4]helicene is open, and interconversion between the enantiomeric forms occurs rapidly under ambient conditions. If bulky substituents are introduced into the helical pitch, stable [4]helicenes can be synthesised.[3] Neutral, nitrogen-centred [4]helicenes have been studied in detail,[4] and cationic, carbon-centred [4]helicenium molecules, conformationally stabilised by methoxy groups in the pitch (Figure 1), have recently gained considerable attention due to their facile synthesis and chiral resolution. [4]Helicenium ions (Figure 1) have been explored as dyes,[5] chiral platforms[6] and also for their unique chemistry.[7,8] [4]Helicenium molecules are synthesised by nucleophilic aromatic substitution (S_NAr),[7e,9] and a similar synthetic pathway was also recently used to synthesise the first [6]helicenium cations.[10] Although [6]helicenium ions have been prepared and reported with aza/aza, aza/oxa and oxa/oxa bridges (X/Y in Figure 1), [4]helicenium ions have proven more elusive as the selectivity of the oxa-bridge formation is low.[9a,b] Nucleophilic insertion and aza-bridge formation of primary amines occur stepwise starting from tris(2,6-dimethoxyphenyl)methylium ($\mathbf{1}^+$, Scheme 1),[11] whereas the dealkylation of methoxy groups and oxa-bridge formation is less well behaved. The aza/aza-bridged [4]helicenium system (R_2-$DMQA^+$, Figure 1) was the first to be synthesised, followed recently by the oxa/oxa-bridged system

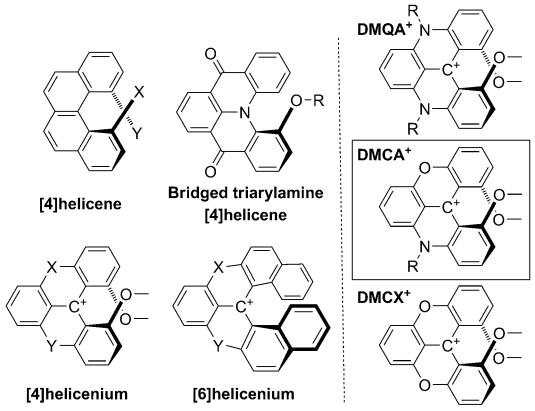

Figure 1. [4]Helicenes and helicenium ions.

[a] *Dr. T. J. Sørensen, Dr. A. Ø. Madsen, Prof. Dr. B. W. Laursen*
Nano-Science Center and Department of Chemistry
University of Copenhagen, Universitetsparken 5
DK2100 København Ø (Denmark)
Fax: (+45) 35-32-02-14
E-mail: bwl@nano.ku.dk

Supporting information for this article is available on the WWW under http://dx.doi.org/10.1002/chem.201400082.

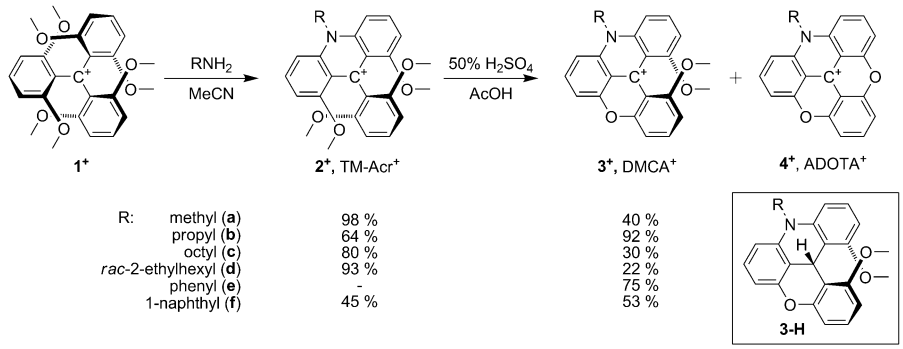

Scheme 1. Synthesis of *N*-alkyl-1,13-dimethoxychromeno[2,3,4-*kl*]acridinium (**3**$^+$, DMCA$^+$).

(DMCX$^+$).[9a,b] In this work we have partially solved the synthetic challenge of the selective oxygen ring closure in the first synthesis of the aza/oxa-bridged derivative *N*-alkyl-1,13-dimethoxychromeno[2,3,4-*kl*]acridinium[12] (**3**$^+$, DMCA$^+$).

Helicenium ions can be viewed as bridged triarylmethylium dyes. Although the flexible parent compounds are non-fluorescent, the locked structures are potent fluorophores.[13] The mono-bridged derivatives, xanthenium and acridinium, bearing donor groups on the periphery, are the best known, that is, the Rhodamine, Fluorescein and Acridine Orange dyes. Because of the cation stability of xanthenium ($pK_{R+} = 2.5$) it has found no applications,[14] whereas acridinium dyes are used as chloride sensors.[15] Helicenium ions are triarylmethylium dyes with two bridges. *N*,*N*′-Dialkyl-1,13-dimethoxyquinolino-[2,3,4-*kl*]acridinium (DMQA$^+$, X = Y = N–R in Figure 1) and 1,13-dimethoxychromeno[2,3,4-*kl*]xanthenium (DMCX$^+$, X = Y = O in Figure 1) are red dyes, with poor-to-mediocre quantum yields.[5,9b] Helicenium ions suffer from solvent-induced quenching, which results in very low quantum yields in polar solvents. This issue is alleviated if a third bridge is introduced. The resulting triangulenium dyes are strong emitters with high quantum yields, highly polarised transitions and long emission lifetimes.[11b,c,16]

Herein we report on the synthesis of six different derivatives of *N*-alkyl-1,13-dimethoxychromeno[2,3,4-*kl*]acridinium (**3**$^+$, DMCA$^+$) and the product of addition of hydride to the central carbon atom. We discuss the cation stability and single-crystal structures of three different derivatives. Finally, the photophysics of the three types of aza/oxa[4]helicenium ions are compared, and the DMQA$^+$ and DMCA$^+$ dye systems are shown to be potential fluorophores in apolar media.

Results and Discussion

Synthesis

Two synthetic pathways to helicenium ions have been reported. A stepwise route, in which a xanthone-like structure is formed and then treated with a carbon nucleophile to incorporate the third arm into the structure,[7e,10] or a direct route, in which the molecular framework is initially formed and then bridged by either external attack by primary amines or internal attack by hydroxy groups released by ether cleaving reagents.[7a,9a,b,d,11c,17] In this work, DMCA$^+$ was synthesised by the second route, as presented in Scheme 1.

Tris(2,6-dimethoxyphenyl)methylium (**1**$^+$) was synthesised as described previously and isolated as its tetrafluoroborate salt.[11b,14] Cation **1**$^+$ was treated with primary amines in acetonitrile to afford *N*-alkyltetramethoxyacridinium **2**$^+$ (TM-Acr, 1,8-dimethoxy-9-(2,6-dimethoxyphenyl)-10-alkylacridinium), which was isolated by precipitation with aqueous potassium hexafluorophosphate or sodium tetrafluoroborate in quantitative yields. Further purification by recrystallisation in methanol, or in the case of **2g** chromatography, yielded analytically pure **2**·PF_6/BF_4 in good-to-excellent yields.

Single ring closure of **2**$^+$ to form **3**$^+$ was achieved by heating **2**$^+$ in a mixture of acetic acid and 50% sulfuric acid. The major byproduct was the fully ring-closed compound azadioxatriangulenium **4**$^+$. To isolate **3**$^+$, chromatography was performed on the neutral centre adduct **3-H** (Scheme 1, inset), acquired by reaction of the crude product obtained above with $NaBH_4$ in DMSO. This allowed easy separation of **3-H** from **4-H** by flash chromatography. Oxidation by using elemental iodine[9a,b] followed by ion exchange resulted in the isolation of the hexafluorophosphate salt of **3**$^+$ in moderate-to-excellent yields. The key steps with regards to the yield are the four precipitations required for the ion exchange. Here, significant amounts of material can be lost. This is particularly problematic with the more lipophilic side-chains, octyl (**2c**) and 2-ethylhexyl (**2d**), and the water-soluble methyl derivative (**2a**).

Unlike the two previously reported [4]helicenium systems (DMQA$^+$ and DMCX$^+$), DMCA$^+$ has no axis of symmetry (Figure 1). As a consequence, the NMR spectrum cannot be readily assigned. Through extensive NMR studies using COSY, NOESY, TOCSY, HMBC and HSQC, the spectrum of **3b** could be fully assigned. The key correlations are shown in Figure 2. Starting from the protons on the α-carbon atom on the N-substituent, NOESY enabled the assignment of the two protons *ortho* to the aza bridge, and NOESY and TOCSY allowed the assignment of the proton that is in a ring system containing a methoxy substituent, and which of the protons with NOE from the proton on the α-carbon on the alkyl chain is on the ring with the aza/oxa bridges. For the full assignment see the Supporting Information. The protons on the aromatic ring with two bridges are the least shielded, and the protons on the aromatic ring with two oxygen substituents are the most efficiently shielded.

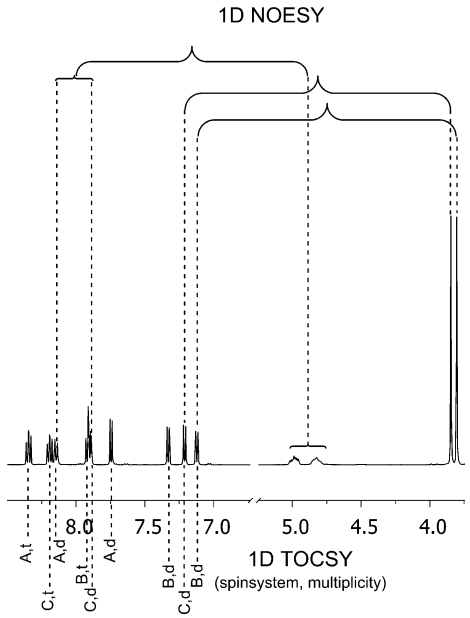

Figure 2. 1D NMR spectrum of **3 b** showing NOESY and TOCSY cross-correlations.

Cation stability and centre adducts

The cation stability is measured by the pK_{R+} value, which reflects the pH at which the cation and carbinol are present in equal quantities.[11b,18] For very stable carbocations, the pH scale can be extended beyond aqueous media by using DMSO/water mixtures containing tetramethylammonium hydroxide and the *C* scale.[11b] The pK_{R+} value is a measure of the stability of the neutral OH centre adduct relative to that of the cation. Figure 3 shows the results of the determination of the cation stability of $DMCA^+$: a value of 13.0 was found. The value is inside the pH range of water, as can be observed as decolouration occurs when $DMCA^+$ is dissolved in concentrated sodium or potassium hydroxide, but determination of pK_{R+} was not possible in highly concentrated alkaline solutions and the *C* scale had to be used.

The thermodynamic stability of a carbocation is to a large extent determined by the ability of the molecular structure to delocalise charge in a conjugated system. The [4]helicenium ions have a twisted conjugation pathway and four electron-donating heteroatoms on which charge can be partially localised, whereas the triangulenium ions have perfectly flat conjugation pathways, but only three heteroatoms in the structure. The cation stabilities of the aza/oxa[4]helicenium and aza/oxatriangulenium ions are compiled in Table 1. A cursory inspection of the data shows that the number of nitrogen atoms in the molecular structure is decisive for cation stability. On closer inspection it can be seen that the more nitrogen bridges there are in the [4]helicenium structure, the less the loss of conjugation (due to twisting) as compared with the stability of the corresponding triangulenium ion.

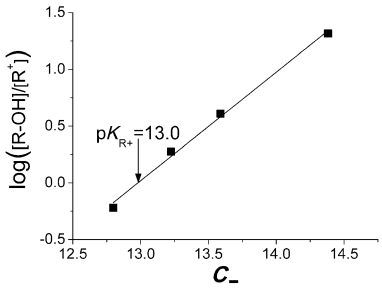

Figure 3. Determination of the cation stability of $DMCA^+$. The concentrations were determined by absorption; Pr-DMCA·PF_6 was used in the experiments.

Table 1. Cation stabilities, measured as pK_{R+}, of the [4]helicenium and triangulenium ions. In all cases the propyl derivatives were used.

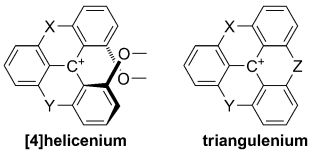

Parent compound	X	Y	Z	pK_{R+}
[4]helicenium	O	O	–	6–8[a]
	N	O	–	13.0[b]
	N	N	–	19.1[c]
triangulenium	O	O	O	9.1[d]
	N	O	O	14.5[e]
	N	N	O	19.4[e]
	N	N	N	23.7[e]

[a] Values from ref. [9b]. [b] Slope of line = 0.957 and corresponding R^2 = 0.994. [c] Values from ref. [8]. [d] Values from ref. [14]. [e] Values from ref. [11b].

Although $DMCX^+$ has a cation stability that is too low for it to be considered a stable species in aqueous solution, $DMCA^+$ will be the dominant species up to pH ≈ 11 ($[ROH] \ll [R^+]$). Whereas $DMQA^+$ and the triangulenium ions with two or three nitrogen bridges are too stable to form the corresponding carbinols in aqueous solution, $DMCA^+$ has a cation stability such that centre adducts can be formed in a polar phase in the presence of a high concentration of nucleophiles and then subsequently be transferred, as a neutral species, to a less polar phase. Thus, the stability of the $DMCA^+$ helicenium ion is in a very attractive range for application as a chiral phase-transfer catalyst.[19]

To investigate the selectivity of the DMCA framework as a potential chiral catalyst, we scrutinised the hydride centre adducts, formed as intermediates in the synthesis of all the derivatives. Furthermore, we chose to investigate the methyl and cyanomethyl adducts of *N*-propyl-$DMCA^+$ (**3 b**). Addition of a nucleophile or hydride to $DMCA^+$ potentially leads to the formation of two diastereomers (see Scheme 2). Lacour and co-workers investigated the diastereoselective addition of nucleophiles (hydride and organolithium) to unsymmetrical $DMQA^+$ helicenium systems having two different peripheral substituents on the two nitrogen atoms in the otherwise symmetrical helical framework.[7a] They assigned the selectivity to

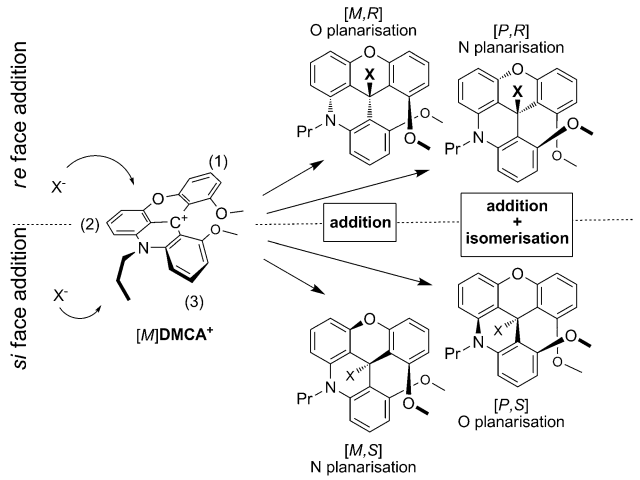

Scheme 2. Structural implications of nucleophilic attack on DMCA$^+$.

Table 2. Selectivity of different derivatives of DMCA$^+$ in reactions with anionic nucleophiles.[a]

Entry	Side-chain	Adduct	d.r.
1	propyl	-CH_3	20:80
2	propyl	-CH_2CN	17:83
3	methyl	-H	17:83
4	propyl	-H	9:91
5	octyl	-H	9:91
6	ethylhexyl	-H	17:83
7	phenyl	-H	25:75
8	naphthyl	-H	20:80

[a] The diastereomeric ratio was determined from the integration of the ^{1}H NMR spectra of the hydrogen atom(s) added to the central carbon atom, see the Supporting Information for examples.

a difference in the structure around the nitrogen atoms, which is dependent on the nature of their substituents, that is, an *N*-alkyl substituent results in a pyramidal nitrogen[16f,g] whereas an *N*-aryl substituent gives a trigonal-planar nitrogen.[16a] If the bulk of the aryl substituent is increased by using mesityl instead of phenyl, the diastereoselectivity can be increased further. Attack of a nucleophile on the [4]helicenium structure can proceed by addition at either the *Re* or *Si* face of the structure (note the terminology is reversed in DMCA$^+$ and DMQA$^+$, see the Supporting Information). For a given helicity (*M*/*P*), attack at a given face must result in planarisation of a given arm of the helical structure. For DMCA$^+$ nucleophilic addition at the *Re* face of the *M* enantiomer will result in planarisation of the xanthene system, whereas addition at the *Si* face will result in a planar acridine system (see Scheme 2). If planarisation of either system is energetically favoured, there will be a marked difference in the thermodynamic stability of the two diastereomers. The kinetic selectivity is expected to be governed by the accessibility of a face, for which the bulk of the substituent on the nitrogen atom will be the critical factor. The work of Lacour and co-workers indicates that kinetic factors, that is, steric bulk, are more important for the diastereoselectivity in the reduction of DMQA$^+$ to H-DMQA than for the addition of organolithium reagents.[7a]

In DMCA$^+$, one side of the molecular structure is open, as the oxygen heteroatom carries no substituent. Based on the results of Lacour and co-workers,[7a] we expected that we would be able to obtain a much higher diastereoselectivity. This assumption is based on the large difference in donor strength between oxygen and nitrogen, which should result in a clear preference for creating a planar acridine system. As it turned out, the data clearly shows that planarisation of the xanthene system is favoured over planarisation of the acridine system, even with aryl substituents on the acridine nitrogen.

The diastereomeric ratios of the centre adducts formed by nucleophilic attack on DMCA$^+$ are shown in Table 2. The data show that the values of d.r. range from 25:75 to 9:91, with the major isomer being the species with a planar xanthene system (see below). The diastereoselectivity is largest in the simple alkyl systems, which indicates that steric bulk is more important for the selectivity than the nature of the nitrogen atom. In fact, trigonal-planar nitrogen atoms with aryl substituents reduce the selectivity.

Scheme 2 also includes the option that the nucleophilic attack is accompanied by inversion of the helicene (isomerisation). However, inversion is not expected to take place as the energy barrier was determined to be around 140 kJ mol^{-1}.[3] Furthermore, the computational study showed that although the barrier to racemisation is reduced upon formation of the centre adduct, this effect is far too small to make this pathway favourable at ambient temperatures.

Molecular structure

We were fortunate that several compounds crystallised, either by recrystallisation or by slow evaporation of solvent from CH_2Cl_2/methanol, CH_2Cl_2/ethanol or CH_2Cl_2/heptane mixtures. Compound **2d**·BF_4 crystallised as a racemate with some disorder in the side-chain, whereas, of the title compounds, *N*-methyl-DMCA·PF_6 (**3a**·PF_6), *N*-propyl-DMCA·PF_6 (**3b**·PF_6) and *N*-phenyl-DMCA·PF_6 (**3e**·PF_6) crystallised neatly, allowing their single-crystal structures to be directly determined. In all cases, both the *M* and *P* isomers were found in the unit cell. Figure 4 shows a single isomer of each of the compounds. Little variation as a function of the side-chain is immediately apparent; the helical structures are close to identical irrespective of the nature of the side chain, and all compounds display a significant helical pitch.

However, significant differences between the three DMCA$^+$ derivatives can be found on closer inspection. Table 3 shows selected crystallographic information, including a measure of the helical pitch and the local structure around the nitrogen atom measured by the out-of-plane displacement (N OOP, for more detailed information and definitions see the Supporting Information). A large difference can be seen between the helical pitches of the alkyl- and aryl-substituted DMCA$^+$ structures, with the pitch of the former being 44.2/44.1° (**3a**/**3b**) and that of the latter reduced to 41.4° (**3e**). The origin of the shallower pitch is not clear, as the nature of the nitrogen atom appears

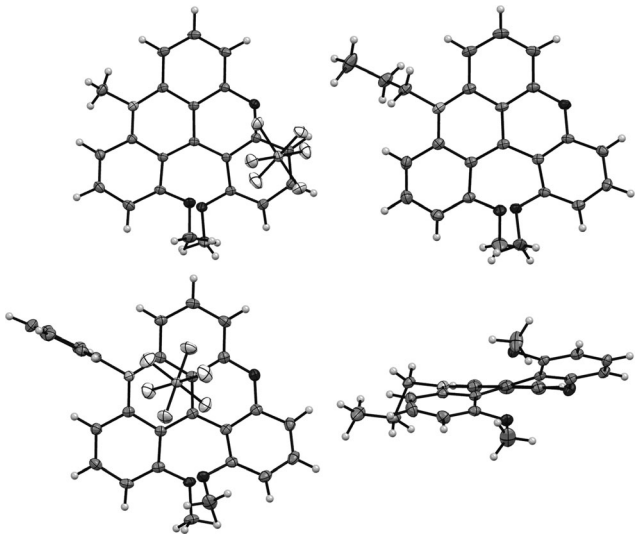

Figure 4. Molecular structures of *N*-methyl-DMCA·PF_6 (**3a**·PF_6; top left), *N*-propyl-DMCA·PF_6 (**3b**·PF_6; top right), *N*-phenyl-DMCA·PF_6 (**3e**·PF_6; bottom left), and *N*-propyl-DMCA·PF_6 (**3b**·PF_6; side view, bottom right) determined by single-crystal diffraction analysis. The structures are shown with ellipsoids drawn at the 50% probability level.

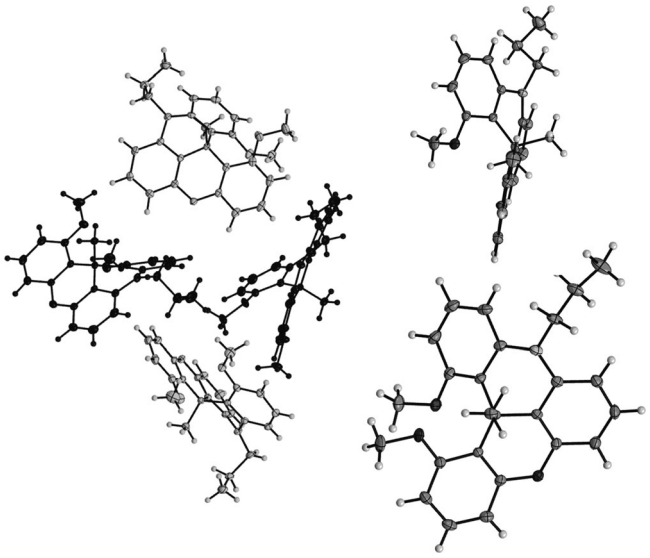

Figure 5. Molecular structures of *N*-propyl-13b-methyl-DMCA (**Me-3b**) determined by single-crystal diffraction analysis. The structures are shown with ellipsoids drawn at the 50% probability level.

Table 3. Selected crystallographic data.

Entry		**3a**·PF_6 methyl	**3b**·PF_6 propyl	**3e**·PF_6 phenyl	**Me-3b** propyl
1	isomer(s)	*P/M*	*P/M*	*P/M*	*M,R*
2	*Z*	4	2	2	4
3	space group	$P2_1/c$	$P\bar{1}$	$P\bar{1}$	$P2_1$
4	pitch[a] [°]	44.16	44.10	41.41	49.01/50.57
5	calcd[a]	46.09	–	–	–
6	N OOP[b]	0.015	0.267	0.031	0.116/0.131

[a] See ref. [3] for details. [b] Nitrogen out-of-plane displacement, as defined in ref. [7a].

not to be related to the shallowness of the pitch. In *N*-methyl-DMCA$^+$ (**3a**) and *N*-phenyl-DMCA$^+$ (**3e**), the nitrogen atom is strictly trigonal planar, whereas in *N*-propyl-DMCA$^+$ (**3b**) it is pyramidal (entry 6, Table 3). If the symmetry of the pitch is measured (see Table S1 in the Supporting Information), it can be concluded that the aryl substituent causes a flattening of the acridinium system compared with the xanthenium system, which results in the smaller pitch observed in the crystal structure of **3e**. Note that the planar-trigonal nitrogen in *N*-methyl-DMCA$^+$ (**3a**) does not lead to a flat acridinium system.

A single isomer (*R,M*) of the centre adduct formed by the addition of methyllithium to *N*-propyl-DMCA·PF_6 (methyl-**3b**) crystallised in the chromatographic eluent. The NMR-scale reaction provided three large crystals suitable for single-crystal X-ray diffraction analysis; unfortunately, only a single data set of sufficiently good quality to determine the structure was obtained. With a d.r. ratio of 20:80, we concluded that the crystal could only consist of one of the enantiomers of the major diastereomeric couple. Four molecules are present in the unit cell occupying two sites (see Figure 5). The structures are significantly different, with different helical pitches and different pitch symmetries (see Table 3 and Table S1 in the Supporting Information). These differences can only be due to packing or crystal effects and highlight the necessity of further studies if the substituent-induced structural perturbations in the [4]helicenium ions are to be elucidated. The key point is that the major diastereomer formed is the one in which the xanthene system is planar (*M,R* or *P,S*). We hope to investigate and document this point further in future work.

Photophysics

As we had all three aza/oxa[4]helicenium ions in hand, we performed a comparative study of their photophysical properties under identical conditions. The data are compiled in Table 4. We have previously published the data for DMCX$^+$,[9b] and the photophysics of DMQA$^+$ has also been examined in detail by Lacour and Vauthey and their co-workers.[5] Excitation spectra and spectra showing the solvatochromism of DMCA$^+$ can be found in the Supporting Information.

Figure 6 shows the absorption spectra of DMCX$^+$, DMCA$^+$ and DMQA$^+$. The first absorption band of the [4]helicenium dyes is redshifted from 580 to 588 to 616 nm, as the number of nitrogen atoms in the molecules increases. Similarly, the molar absorptivity increases from 3100 to 9000 to 18100 $M^{-1}cm^{-1}$. The main absorption band involves the entire conjugated system and it is evident that the oxygen donors are not as directly involved as the nitrogen donors. The second band at around 550 nm primarily involves the transfer of electron density from the methoxy-substituted aromatic rings;[5] these are of a similar energy for all three species irrespective of the nature of the electron donors. The band at around 450 nm is strong in all spectra and corresponds to a local transition in the xanthenium and acridinium systems. As xanthenium is a better chromophore than acridinium, the band is strongest

Table 4. Photophysical properties of DMCX·PF_6,[a] *N*-propyl-DMCA·PF_6 and *N,N'*-dipropyl-DMQA·BF_4[b] in various solvents.

[4]Helicenium ion	Solvent	λ_{max} [nm]	ε[c] [$cm^{-1}\,M^{-1}$]	λ_{fl} [nm]	Stokes' shift [cm^{-1}]	ϕ_{fl}[d] [%]	τ_{fl} [ns] (amplitude contribution [%])	$\tau_{av,ampl}$ [ns]
Pr_2DMQA^+	CH_2Cl_2	616	18100	650	850	33	11.4	11.4
	MeCN	615	17500	661	1130	8	3.5 (79) 7.2 (21)	4.6
	H_2O/DMSO[e]	618	15000	666	1170	2	1.5 (67) 9.4 (33)	4.1
$PrDMCA^+$	CH_2Cl_2	588	9000	623	960	22	12.0	12
	MeCN	584	8400	630	1250	6	4.2 (99) 13 (1)	4.3
	MeOH	583	8800	628	1230	5	3.7 (99) 14 (1)	3.9
$PhDMCA^+$	CH_2Cl_2	599	9400	630	820	18	10.2	10.2
	MeCN	592	8800	633	1090	5	3.4 (99) 11 (1)	3.5
	MeOH	591	10600	634	1150	3	3.1 (99) 12 (1)	3.2
$DMCX^+$	CH_2Cl_2	50	3100	613	930	2	2.3	2.3
	MeCN	570	2900	615	1280	0.05	--[f]	--[f]

[a] See ref. [9b]. [b] See ref. [8]. [c] An experimental error of 10% is assumed. [d] A minimum error of 5% is assumed. Determined by using Cresyl Violet as reference ($\Phi_{fl.}=0.54$, MeOH).[20] [e] 95% water with 5% DMSO. [f] Could not be determined due to the very low intensity.

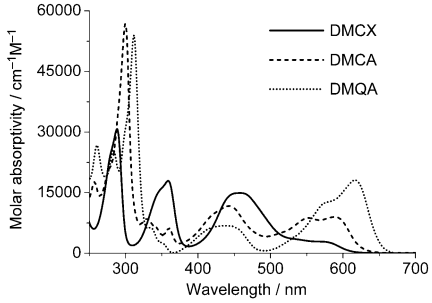

Figure 6. Absorption spectra of the [4]helicenium ions in acetonitrile. Concentrations are kept below 10^{-4} M.

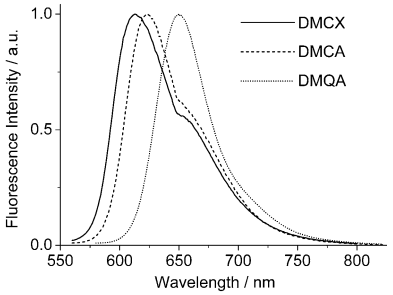

Figure 7. Emission spectra of the [4]helicenium ions in acetonitrile following excitation at 545 (DMCX), 550 (DMCA) and 448 nm (DMQA). Concentrations are kept below 10^{-5} M.

in $DMCX^+$. The bands at higher energies arise from transitions localised in the chromeno and quinolino substructures.

Figure 7 shows the emission spectra of the [4]helicenium dyes. As for the absorption maximum, the emission maximum is redshifted from 613 to 623 to 650 nm as the number of nitrogen donors in the structures increases. The Stokes' shift is identical at 35 nm (820–960 cm^{-1}) for the three dyes. The emission maximum of $DMCA^+$ is not solvent-dependent, but increases with solvent polarity for $DMQA^+$. The fluorescence quantum yield is highly solvent-dependent for all the [4]helicenium ions (Table 4). If the values determined in CH_2Cl_2 are compared, $DMQA^+$ is the most emissive with $\phi_{fl}=33\%$, followed by $DMCA^+$ with $\phi_{fl}=22\%$ and $DMCX^+$ with $\phi_{fl}=2\%$. The fluorescence lifetimes are long in all systems, as expected for medium-strength oscillators.[21]

If the solvatochromism of the [4]helicenium ions is compared, minor shifts in band positions and widths are found. The energetics of the electronic states of the ions are not strongly perturbed by the solvent. Table 4 includes the quantum yields determined for $DMCX^+$, $DMCA^+$ and $DMQA^+$ in different solvents. It is evident that the kinetics governing the depopulation of the excited states in the dyes are strongly influenced by the solvent, and particularly by the solvent polarity. The decay kinetics become multi-exponential in polar solvents, which suggests multiple populations or conformations present in solution. The exact mechanism of the solvent-induced quenching is still not known.

To study the effect of the nitrogen substituent, the photophysical properties of *N*-propyl-$DMCA^+$ (**3b**) and *N*-phenyl-$DMCA^+$ (**3e**) were studied. Note that the solid-state structures of the two compounds are significantly different. The nitrogen donor in *N*-phenyl-$DMCA^+$ is fully sp^2-hybridised, whereas it has a greater degree of sp^3 character in *N*-propyl-$DMCA^+$. This should be evident in the spectra. The introduction of a phenyl group instead of a propyl group is followed by a 10 nm redshift of the absorption and emission, which confirms our assumption. A slight increase in molar absorptivity and a shortening of the fluorescence lifetime indicate that *N*-phenyl-$DMCA^+$ is a marginally stronger chromophore. Similar effects were observed to have a large impact on the dye properties of phenyl-substituted triazatriangulenium ($TATA^+$).[16a] However, in this case the effect on the quantum yield is small and should be treated with caution.

Conclusion

We have developed an efficient route for the synthesis of *N*-alkyl-1,13-dimethoxychromeno[2,3,4-*kl*]acridinium ($DMCA^+$), and have tested it by synthesising six different derivatives. The cation stability of the $DMCA^+$ structure was determined to be $pK_{R+} = 13.0$. As a consequence, $DMCA^+$ ions are stable in aqueous media, but can be forced to the neutral carbinol form at high pH. The chiral nature of the [4]helicenium structure was investigated through the formation of adducts at the central carbon atom. This resulted in diastereomeric molecules that could be differentiated by NMR spectroscopy, and the diastereomeric ratios were found to range between 25:75 and 9:91 depending on the *N*-substituent. The mechanism for the stereoselectivity has been discussed.

The single-crystal structures and photophysical properties of $DMCA^+$ were studied. In the solid-state, the nitrogen substituent changes the local structure around the nitrogen atom, and the absorption and emission bands are redshifted by 10 nm when an *N*-alkyl substituent is replaced by an *N*-aryl substituent. $DMCA^+$ was shown to be a red dye with a moderate quantum yield in apolar solvents and a poor quantum yield in polar solvents. The reason for the solvent-induced quenching is a subject for further study.

Experimental Section

General

Chemicals and solvents were used as received. The synthesis of tris(2,6-dimethoxyphenyl)carbenium tetrafluoroborate (**1**) was adapted from refs. [8,11b,14]. Detailed information on the experimental procedures involved in the determination of pK_{R+} values can be found in ref. [11b]. Absorption spectra were recorded on a Perkin–Elmer Lambda 1050 spectrophotometer in cuvettes with a pathway of 1 cm. Fluorescence excitation and emission spectra were recorded in a conventional L-shaped configuration on a Horiba Fluorolog 3 spectrofluorimeter equipped with an analogue TC-SPC accessory.

Crystallography

Single crystals were selected by using a polarising microscope. Diffraction data were collected on a Nonius–KappaCCD diffractometer with graphite-monochromated Mo K_α radiation. The temperature was maintained at 122.4(5) K by using an Oxford Cryosystems low-temperature liquid nitrogen cooling device. Data reduction was performed by using the Nonius COLLECT suite of programs.[22] The structures were obtained by direct methods using SHELXS-97 and refined by full-matrix least-squares methods against F^2 using the SHELXL-97 program.[23] Positions and anisotropic displacement parameters were refined for all non-hydrogen atoms. Hydrogen atoms were located based on difference maps and their positions and isotropic displacement parameters were refined. Given the use of Mo radiation, the absolute configuration of the chiral crystal **Me-3b** could not be determined. Details about the data collection, structure determination and structures are given the Supporting Information.

CCDC- 922657 (**2d**·BF_4), -922660 (**3a**·PF_6), -922658 (**3b**·PF_6), -922659 (**3e**·PF_6) and -922661 (**Me-3b**) contain the supplementary crystallographic data for this paper. These data can be obtained free of charge from The Cambridge Crystallographic Data Centre via www.ccdc.cam.ac.uk/data_request/cif.

Synthesis

General procedure for the preparation of 10-substituted 1,8-dimethoxy-9-(2,6-dimethoxyphenyl)acridinium hexafluorophosphate (2): Tris(2,6-dimethoxyphenyl)carbenium tetrafluoroborate (**1**; 1 g, 2 mmol) was dissolved in acetonitrile (50 mL) and amine (4 equiv) was added. The reaction mixture was stirred for 2 h after which the reaction mixture was poured into 0.2 M aqueous KPF_6 (400 mL). The crude product was collected by filtration and recrystallised from methanol (100 mL g^{-1}).

1,8-Dimethoxy-9-(2,6-dimethoxyphenyl)-10-methylacridinium hexafluorophosphate (2a): Yield: 5.5 g (98%); dark-red powder. ^{1}H NMR (500 MHz, DMSO): $\delta = 8.26$ (dd, $J = 9.1$, 8.0 Hz, 2H), 8.15 (d, $J = 8.7$ Hz, 2H), 7.44 (t, $J = 8.4$ Hz, 1H), 7.21 (d, $J = 7.9$ Hz, 2H), 6.81 (d, $J = 8.4$ Hz, 2H), 4.72 (s, 3H), 3.53 (s, 3H), 3.52 ppm (s, 3H); ^{13}C NMR (126 MHz, DMSO): $\delta = 159.69$, 155.64, 155.28, 141.87, 139.55, 129.24, 119.10, 119.05, 110.25, 106.72, 103.69, 57.10, 55.81, 40.65 ppm; UV/Vis (MeCN): λ [log (ε/M^{-1}cm^{-1})] = 530 sh [3.60], 497 [3.70], 467 sh [3.60], 397 [3.78], 356 [3.40], 337 [3.18], 286 [4.9], 246 nm [4.29]; elemental analysis calcd (%) for $C_{24}H_{24}NO_4PF_6$: C 53.84, H 4.52, N 2.62; found: C 53.81, H 4.45, N 2.52.

1,8-Dimethoxy-9-(2,6-dimethoxyphenyl)-10-propylacridinium hexafluorophosphate (2b): Yield: 5.8 g (64%); dark-red needles. ^{1}H NMR (500 MHz, DMSO): $\delta = 8.27$ (t, $J = 8.6$ Hz, 2H), 8.12 (d, $J = 9.2$ Hz, 2H), 7.43 (t, $J = 8.4$ Hz, 1H), 7.22 (d, $J = 8.0$ Hz, 2H), 6.81 (d, $J = 8.4$ Hz, 2H), 5.15 (m, 2H), 3.53 (s, 6H), 3.52 (s, 6H), 2.11 (m, 2H), 1.22 ppm (t, $J = 7.3$ Hz, 3H); ^{13}C NMR (126 MHz, DMSO): $\delta = 159.92$, 155.98, 155.25, 140.96, 140.02, 129.26, 119.12, 119.06, 109.75, 106.82, 103.67, 57.11, 55.85, 53.15, 21.16, 10.64 ppm; UV/Vis (MeCN): λ [log (ε/M^{-1}cm^{-1})] = 530 sh [3.60], 497 [3.70], 467 sh [3.60], 397 [3.78], 356 [3.40], 337 [3.18], 286 [4.9], 246 nm [4.29]; elemental analysis calcd (%) for $C_{26}H_{28}NO_4PF_6$: C 55.42, H 5.01, N 2.49;found: C 55.44, H 4.98, N 2.36.

1,8-Dimethoxy-9-(2,6-dimethoxyphenyl)-10-octylacridinium tetrafluoroborate (2c): Yield: 900 mg (80%); red powder. ^{1}H NMR (500 MHz, DMSO): $\delta = 8.28$ (dd, $J = 9.1$, 8.0 Hz, 2H), 8.09 (d, $J = 9.2$ Hz, 2H), 7.43 (t, $J = 8.4$ Hz, 1H), 7.22 (d, $J = 8.0$ Hz, 2H), 6.81 (d, $J = 8.4$ Hz, 2H), 5.18 (m, 2H), 3.53 (s, 6H), 3.52 (s, 6H), 2.06 (m, 2H), 1.66 (dt, $J = 15.3$, 7.7 Hz, 2H), 1.42 (dt, $J = 14.6$, 6.8 Hz, 2H), 1.34 (m, 2H), 1.29 (m, 4H), 0.88 ppm (t, $J = 6.9$ Hz, 3H); ^{13}C NMR (126 MHz, DMSO): $\delta = 159.94$, 155.96, 155.25, 140.92, 140.06, 129.26, 119.14, 119.07, 109.66, 106.82, 103.68, 57.11, 55.83, 51.91, 31.20, 28.68, 28.66, 27.75, 25.85, 22.07, 13.96 ppm; UV/Vis (MeCN): λ [log (ε/M^{-1}cm^{-1})] = 530 sh [3.60], 497 [3.70], 467 sh [3.60], 397 [3.78], 356 [3.40], 337 [3.18], 286 [4.9], 246 ppm [4.29]; elemental analysis calcd (%) for $C_{26}H_{28}NO_4BF_4$: C 64.70, H 6.66, N 2.43; found: C 64.67, H 6.69, N 2.36.

1,8-Dimethoxy-9-(2,6-dimethoxyphenyl)-10-(2-ethylhexyl)-acridinium tetrafluoroborate (2d): Yield: 2.1 g (93%); orange needles. ^{1}H NMR (500 MHz, $CDCl_3$): $\delta = 8.38$ (dd, $J = 180.7$, 171.9 Hz, 2H), 7.94 (d, $J = 9.1$ Hz, 2H), 7.37 (t, $J = 8.4$ Hz, 1H), 7.02 (d, $J = 8.0$ Hz, 2H), 6.66 (d, $J = 8.4$ Hz, 2H), 5.22 (dd, $J = 7.8$, 1.0 Hz, 2H), 3.57 (s, 6H), 3.56 (s, 6H), 2.26 (m, 1H), 1.54 (m, 2H), 1.45–1.5 (m, 6H), 0.94 (t, $J = 7.4$ Hz, 3H), 0.81 ppm (t, $J = 7.2$ Hz, 3H); ^{13}C NMR (126 MHz, $CDCl_3$): $\delta = 160.89$, 157.44, 142.45, 140.12, 140.09, 129.66,

120.29, 119.75, 109.92, 106.61, 103.56, 57.08, 56.19, 55.38, 39.73, 30.60, 28.80, 24.24, 23.03, 14.05, 11.18 ppm; UV/Vis (MeCN): λ [log (ε/M^{-1}cm^{-1})] = 534 sh [3.56], 500 [3.64], 468 sh [3.54], 400 [3.72], 356 [3.25], 337 [3.11], 286 [4.9], 246 nm [4.18]; elemental analysis calcd (%) for $C_{26}H_{28}NO_4BF_4$: C 64.70, H 6.66, N 2.43; found: C 64.76, H 6.75, N 2.35.

1,8-Dimethoxy-9-(2,6-dimethoxyphenyl)-10-phenylacridinium hexafluorophosphate (2e): Acridinium salt 2e was prepared as described in the literature.[24]

1,8-Dimethoxy-9-(2,6-dimethoxyphenyl)-10-(1-naphthyl)acridinium tetrafluoroborate (2f): Purified by chromatography with EtOAc as eluent. Yield: 430 mg (45%); dark-brown powder. ^{1}H NMR (500 MHz, $CDCl_3$): δ = 8.33 (d, J = 8.4 Hz, 1H), 8.16 (d, J = 8.3 Hz, 1H), 7.89 (dd, J = 8.3, 7.4 Hz, 1H), 7.83 (dd, J = 9.0, 8.0 Hz, 2H), 7.68 (d, J = 8.2 Hz, 1H), 7.65 (m, 1H), 7.44 (m, 2H), 7.02 (d, J = 7.9 Hz, 2H), 6.76–6,66 (m, 5H), 3.69 (s, 3H), 3.66 (s, 3H), 3.62 ppm (s, 6H); ^{13}C NMR (126 MHz, $CDCl_3$): δ = 160.98, 160.44, 155.92, 155.77, 142.96, 140.50, 135.17, 134.65, 132.39, 130.20, 129.53, 129.49, 128.43, 128.40, 126.87, 126.63, 121.08, 119.93, 119.11, 110.68, 107.02, 103.76, 103.67, 57.32, 56.38, 56.30 ppm; UV/Vis (MeCN): λ [log (ε/M^{-1}cm^{-1})] = 542 sh [3.59], 506 [3.67], 476 sh [3.59], 406 [3.68], 355 [3.46], 336 [3.35], 286 [4.9], 247 nm [4.27]; elemental analysis calcd (%) for $C_{33}H_{28}NO_4BF_4$: C 61.21, H 4.36, N 2.16; found: C 61.20, H 4.39, N 2.19.

General procedure for the preparation of N-substituted 1,13-dimethoxychromeno[2,3,4-*kl*]acridinium hexafluorophosphate (3): 10-Substituted 1,8-dimethoxy-9-(2,6-dimethoxyphenyl)acridinium hexafluorophosphate (**2**; 1 mmol) was dissolved in acetic acid (50 mL) and 50% sulfuric acid (25 mL) was added. The reaction mixture was heated at reflux until the stating material peak in the MALDI-TOF mass spectrum had disappeared (24–36 h). The hot reaction mixture was poured into 0.2 M aqueous KPF_6 (400 mL). The crude product was collected by filtration and was directly washed off the filter by using DMSO (50 mL). $NaBH_4$ (250 mg) was then added to the DMSO solution. After 10 min, the reaction mixture was poured into water (200 mL) and the colourless neutral product was extracted with diethyl ether (3×150 mL). The combined organic extracts were pooled and washed with water (3×200 mL), dried over $MgSO_4$ and the solvent was removed. Column chromatography on silica 60 (0.063–0.200 mm) with 5 vol% diethyl ether in *n*-heptane gave the reduced product **3-H** as a white crystalline material. The pure hydride adduct was taken up in diethyl ether (50 mL) and I_2 (1 g in 100 mL diethyl ether) was added. The mixture was stirred for 1 h and then the I_3^- salt of the product was collected and taken up in acetonitrile. The PF_6^- salt was precipitated by the addition of 0.2 M aqueous KPF_6 (600 mL) and collected by filtration. The precipitation was repeated twice. After the final precipitation, the product purity was determined by UV/Vis spectroscopy. If the spectrum showed any sign of I_3^- absorption (ca. 300 nm), the crude product was taken up in CH_2Cl_2 and washed with 0.2 M aqueous KPF_6 (4×200 mL) and water (2×200 mL). The CH_2Cl_2 phase was dried over $MgSO_4$ and concentrated in vacuo. The product was precipitated with *n*-heptane and collected by filtration.

***N*-Methyl-1,13-dimethoxychromeno[2,3,4-*kl*]acridinium triiodide (3a)**: Prepared as the triiodide salt. Yield: 1.1 g (40%); dark-red powder. ^{1}H NMR (500 MHz, DMSO): δ = 8.33 (dd, J = 8.8, 8.1 Hz, 1H), 8.19 (dd, J = 9.0, 8.0 Hz, 1H), 8.11 (m, 1H), 7.91 (t, J = 8.4 Hz, 1H), 7.87 (d, J = 9.0 Hz, 1H), 7.73 (dd, J = 8.0, 0.5 Hz, 1H), 7.33 (dd, J = 8.4, 0.9 Hz, 1H), 7.21 (d, J = 7.9 Hz, 1H), 7.12 (dd, J = 8.4, 0.7 Hz, 1H), 4.44 (s, 3H), 3.84 (s, 3H), 3.80 ppm (s, 3H); ^{13}C NMR (126 MHz, DMSO): δ = 159.49, 158.92, 155.15, 149.94, 143.71, 143.14, 139.63, 138.88, 137.69, 137.37, 116.31, 113.84, 110.87, 110.20, 108.82, 108.65, 108.27, 106.39, 104.30, 56.23, 38.53 ppm; UV/Vis (MeCN): λ [log (ε/M^{-1}cm^{-1})] = 591 [3.92], 557 [3.91], 435 sh [3.91], 360 [4.13], 297 nm [4.71]; HRMS (ESI-TOF): *m/z* calcd for $C_{22}H_{18}NO_3^+$: 344.1287; found: 344.1281. elemental analysis calcd (%) for $C_{22}H_{18}NO_3I_3$: C 36.44, H 2.50, N 1.93; found: C 36.45, H 2.29, N 1.78.

***N*-Propyl-1,13-dimethoxychromeno[2,3,4-*kl*]acridinium hexafluorophosphate (3b)**: Yield: 300 mg (92%); dark-red powder.^{1}H NMR (500 MHz, DMSO): δ = 8.33 (dd, J = 8.8, 8.1 Hz, 1H), 8.18 (dd, J = 9.0, 8.0 Hz, 1H), 8.13 (d, J = 8.9 Hz, 1H), 7.91 (t, J = 8.4 Hz, 1H), 7.88 (d, J = 9.1 Hz, 1H), 7.73 (d, J = 7.9 Hz, 1H), 7.32 (dd, J = 8.4, 0.8 Hz, 1H), 7.20 (d, J = 8.0 Hz, 1H), 7.11 (d, J = 7.8 Hz, 1H), 4.97 (m, 1H), 4.81 (m, 1H), 3.83 (s, 3H), 3.79 (s, 3H), 2.02 (d, J = 2.7 Hz, 2H), 1.17 ppm (s, 3H); ^{13}C NMR (126 MHz, DMSO): δ = 159.83, 158.90, 155.15, 150.17, 143.30, 142.93, 139.82, 138.11, 137.67, 137.57, 116.42, 113.80, 110.88, 109.93, 108.82, 108.39, 108.37, 106.34, 104.08, 56.22, 51.41, 40.01, 39.93, 39.84, 39.76, 39.67, 39.51, 39.34, 39.17, 39.01, 20.60, 10.77 ppm; UV/Vis (MeCN): λ [log (ε/M^{-1}cm^{-1})] = 584 [3.92], 550 [3.91], 437 [4.07], 361 [3.81], 340 sh [3.78], 324 [3.95], 298 [4.80], 256 nm [4.26]; HRMS (ESI-TOF): *m/z* calcd for $C_{24}H_{22}NO_3^+$: 372.1594; found: 372.1587; elemental analysis calcd (%) for $C_{24}H_{22}NO_3PF_6$: C 55.71, H 4.29, N 2.71; found C, 55.65, H 4.16, N 2.51.

***N*-Octyl-1,13-dimethoxychromeno[2,3,4-*kl*]acridinium hexafluorophosphate (3c)**: Yield: 310 mg (30%); dark-red powder. ^{1}H NMR (500 MHz, $CDCl_3$): δ = 8.24 (dd, J = 8.7, 8.2 Hz, 1H), 8.17 (dd, J = 9.0, 8.1 Hz, 1H), 7.79 (m, 1H), 7.79 (t, J = 8.3 Hz, 1H), 7.59 (t, J = 9.1 Hz, 2H), 7.22 (dd, J = 8.4, 0.9 Hz, 1H), 7.04 (d, J = 8.0 Hz, 1H), 6.89 (d, J = 7.8 Hz, 1H), 4.94 (m, 1H), 4.78 (m, 1H), 3.89 (s, 3H), 3.84 (s, 3H), 2.15 (m, 2H), 1.71 (m, 2H), 1.38 (m, 2H), 1.32 (m, 6H), 0.91 ppm (s, 3H); ^{13}C NMR (126 MHz, DMSO): δ = 159.84, 158.88, 155.14, 150.17, 143.25, 142.88, 139.85, 138.05, 137.67, 137.61, 116.43, 113.83, 110.87, 109.86, 108.81, 108.39, 108.30, 106.35, 104.08, 56.22, 49.96, 31.17, 28.69, 28.65, 27.18, 25.96, 22.05, 13.95 ppm; UV/Vis (MeCN): λ [log (ε/M^{-1}cm^{-1})] = 584 [3.92], 550 [3.91], 437 [4.07], 361 [3.81], 340 sh [3.78], 324 [3.95], 298 [4.80], 256 nm [4.26]; HRMS (ESI-TOF): *m/z* calcd for $C_{29}H_{32}NO_3^+$: 442.2377; found: 442.2379.

***N*-(*rac*-2-Ethylhexyl)-1,13-dimethoxychromeno[2,3,4-*kl*]acridinium hexafluorophosphate (3d)**: Yield: 180 mg (22%); dark-red powder. ^{1}H NMR (500 MHz, DMSO): δ = 8.34 (t, J = 8.4 Hz, 1H), 8.22 (d, J = 7.1 Hz, 1H), 8.18 (dd, J = 9.0, 8.1 Hz, 1H), 7.91 (t, J = 8.4 Hz, 1H), 7.88 (m, 1H), 7.74 (d, J = 8.0 Hz, 1H), 7.33 (dd, J = 8.4, 0.8 Hz, 1H), 7.20 (d, J = 8.0 Hz, 1H), 7.11 (d, J = 8.5 Hz, 1H), 5.05 (m, 2H), 3.83 (s, 3H), 3.80 (s, 1.5H), 3.79 (s, 1.5H), 1.99 (br s, 1H), 1.54–0.92 (m, 8H), 0.91–0.45 ppm (m, 6H); ^{13}C NMR (126 MHz, DMSO): δ = 158.90, 155.21, 155.19, 150.18, 150.13, 143.55, 143.42, 143.30, 139.69, 137.82, 137.41, 116.56, 116.53, 110.90, 110.87, 110.69, 108.84, 108.45, 106.40, 106.38, 104.08, 56.35, 56.28, 56.20, 51.63, 38.08, 29.15, 27.31, 23.01, 22.00, 13.25, 10.37 ppm; UV/Vis (MeCN): λ [log (ε/M^{-1}cm^{-1})] = 584 [3.92], 550 [3.91], 437 [4.07], 361 [3.81], 340 sh [3.78], 324 [3.95], 298 [4.80], 256 nm [4.26]; HRMS (ESI-TOF): *m/z* calcd for $C_{29}H_{32}NO_3^+$: 442.2377; found: 442.2371; elemental analysis calcd (%) for $C_{29}H_{32}NO_3PF_6 \cdot {}^1/_2CH_2Cl_2$: C 56.24, H 5.28, N 2.22; found: C 56.37, H 5.22, N 2.11.

***N*-Phenyl-1,13-dimethoxychromeno[2,3,4-*kl*]acridinium hexafluorophosphate (3e)**: Yield: 460 mg (75%); dark-red powder.

^{1}H NMR (500 MHz, $CDCl_3$): δ = 8.00 (dd, J = 8.7, 8.1 Hz, 1H), 7.91 (dd, J = 8.9, 8.0 Hz, 1H), 7.87–7.78 (m, 4H), 7.58 (dd, J = 8.9, 1.3 Hz, 1H), 7.57 (dd, J = 8.0, 0.7 Hz, 1H), 7.50 (dt, J = 3.2, 1.3 Hz, 1H), 7.24 (d, J = 0.9 Hz, 1H), 7.05 (d, J = 7.8 Hz, 1H), 6.96 (d, J = 8.1 Hz, 2H), 6.74 (dd, J = 8.9, 0.6 Hz, 1H), 3.94 (s, 3H), 3.90 ppm (s, 3H); ^{13}C NMR (126 MHz, $CDCl_3$): δ = 160.66, 159.99, 156.73, 151.34, 146.45, 145.06, 140.47, 139.79, 138.57, 137.32, 132.48, 131.65, 131.57, 128.89, 128.13, 116.58, 114.33, 112.29, 110.68, 109.72, 109.68, 109.14, 106.46, 104.84, 56.93, 56.80 ppm; UV/Vis (MeCN): λ [log (ε/M^{-1}cm^{-1})] = 592 [3.92], 555 [3.91], 442 [4.07], 361 [3.81], 341 sh [3.85], 329 [3.95], 299 [4.73], 257 nm [4.26]; HRMS (ESI-TOF): m/z calcd for $C_{27}H_{20}NO_3^+$: 406.1438; found: 406.1432; elemental analysis calcd (%) for $C_{27}H_{20}NO_3PF_6 \cdot {}^1/_4CH_2Cl_2$: C 57.15, H 3.61, N 2.54; found: C 57.10, H 3.45, N 2.48.

***N*-(1-Naphthyl)-1,13-dimethoxychromeno[2,3,4-*kl*]acridinium hexafluorophosphate (3f)**: Yield: 100 mg (53%); dark-red powder. Major: ^{1}H NMR (500 MHz, DMSO): δ = 8.44 (d, J = 8.1 Hz, 1H), 8.30 (d, J = 8.3 Hz, 1H), 8.05 (m, 1H), 7.98 (m, 2H), 7.93 (m, 1H), 7.87 (dd, J = 8.7, 8.2 Hz, 1H), 7.72 (dd, J = 14.1, 7.5 Hz, 2H), 7.48 (dd, J = 11.2, 4.1 Hz, 1H), 7.41 (d, J = 8.4 Hz, 1H), 7.27 (d, J = 8.4 Hz, 1H), 7.19 (t, J = 8.2 Hz, 2H), 6.67 (d, J = 8.8 Hz, 1H), 6.45 (d, J = 8.9 Hz, 1H), 3.91 (s, 3H), 3.87 ppm (s, 3H); ^{13}C NMR (126 MHz, DMSO): δ = 160.13, 159.40, 155.72, 150.33, 145.58, 144.49, 140.06, 139.62, 138.46, 137.89, 134.41, 133.99, 131.63, 129.16, 128.81, 128.64, 127.78, 127.12, 126.82, 121.86, 116.65, 113.84, 111.18, 110.53, 109.03, 109.03, 108.48, 106.63, 104.44, 56.41, 56.38 ppm; UV/Vis (MeCN): λ [log (ε/M^{-1}cm^{-1}] = 592 [3.92], 555 [3.91], 442 [4.07], 361 [3.81], 341 sh [3.85], 329 [3.95], 299 [4.73], 257 nm [4.26]. HRMS (ESI-TOF): m/z calcd for $C_{31}H_{22}NO_3^+$: 456.1600; found: 456.1616.

***N*-Propyl-1,13-dimethoxy-13b-methylchromeno[2,3,4-*kl*]acridine (Me-3b)**: Acridine **Me-3b** was prepared as described in ref. [7a]. Major diastereomer: ^{1}H NMR (500 MHz, $CDCl_3$): δ = 7.19 (t, J = 8.2 Hz, 1H), 7.10 (td, J = 8.1, 1.9 Hz, 2H), 6.79 (dd, J = 8.3, 0.8 Hz, 1H), 6.73 (d, J = 8.2 Hz, 1H), 6.68 (m, 2H), 6.59 (dd, J = 8.2, 1.1 Hz, 1H), 6.51 (dd, J = 8.1, 0.8 Hz, 1H), 3.97 (pd (quintet of doublets), J = 14.1, 6.2 Hz, 2H), 3.81 (s, 3H), 3.34 (s, 3H), 1.99 (m, 2H), 1.69 (s, 3H), 1.08 ppm (t, J = 7.4 Hz, 3H). Minor diastereomer: ^{1}H NMR (500 MHz, $CDCl_3$): δ = 7.19 (m, 1H), 7.07 (m, 2H), 6.91 (dt, J = 10.1, 5.1 Hz, 1H), 6.73 (m, 1H), 6.68 (d, J = 0.4 Hz, 2H), 6.55 (d, J = 7.9 Hz, 1H), 6.51 (m, 1H), 3.97 (pd, J = 14.1, 6.2 Hz, 2H), 3.78 (s, 3H), 3.39 (s, 3H), 1.84 (s, 3H), 1.80 (dd, J = 15.5, 7.8 Hz, 2H), 1.05 ppm (t, J = 7.5 Hz, 3H).

***N*-Propyl-13b-cyanomethyl-1,13-dimethoxychromeno[2,3,4-*kl*]-acridine ($NCCH_2$-3b)**: Acridine **$NCCH_2$-3b** was synthesised as described in ref. [8]. Major diastereomer: ^{1}H NMR (500 MHz, DMSO): δ = 7.34 (dd, J = 16.8, 8.4 Hz, 1H), 7.21 (m, 2H), 6.97 (d, J = 8.1 Hz, 1H), 6.92 (d, J = 8.0 Hz, 1H), 6.77 (m, 3H), 6.64 (m, 1H), 4.02 (m, 2H), 3.78 (m, 4H), 3.36 (m, 3H), 3.22 (d, J = 16.7 Hz, 1H), 1.05 ppm (d, J = 7.3 Hz, 3H). Minor diastereomer: ^{1}H NMR (500 MHz, DMSO): δ = 7.45 (t, J = 8.2 Hz, 1H), 7.22 (s, 1H), 7.12 (s, 1H), 7.05 (d, J = 8.1 Hz, 1H), 6.88 (d, J = 8.3 Hz, 1H), 6.77 (m, 3H), 6.64 (m, 1H), 4.02 (m, 2H), 3.76 (s, 3H), 3.69 (d, J = 17.1 Hz, 1H), 3.39 (s, 3H), 2.88 (d, J = 16.7 Hz, 1H), 1.00 ppm (s, 3H).

Acknowledgements

The Danish Research Council for Independent Research | Natural Sciences (instrument grant no. #09-066663), the Danish Research Council for Independent Research | Technology and Production Sciences (grant no. #10-093546) and the Danish National Research Foundation under the Danish–Chinese Centre for Self-Assembled Molecular Electronic Nanosystems are gratefully acknowledged for financial support.

Keywords: carbocations · fluorescence · helical structures · organic dyes · X-ray diffraction

[1] For recent reviews, see: a) Y. Shen, C.-F. Chen, *Chem. Rev.* **2012**, *112*, 1463–1535; b) M. Gingras, *Chem. Soc. Rev.* **2013**, *42*, 968–1006; c) M. Gingras, G. Felix, R. Peresutti, *Chem. Soc. Rev.* **2013**, *42*, 1007–1050; d) M. Gingras, *Chem. Soc. Rev.* **2013**, *42*, 1051–1095; e) A. Urbano, M. C. Carreno, *Org. Biomol. Chem.* **2013**, *11*, 699–708; f) N. Hoffmann, *J. Pharm. Res. Dev. J. Photochem. Photobiol. C: Photochem. Rev.* **2014**, *19*, 1–19.

[2] For recent examples, see: a) A. Latorre, A. Urbano, M. C. Carreno, *Chem. Commun.* **2009**, *0*, 6652–6654; b) L. Severa, D. Koval, P. Novotna, M. Oncak, P. Sazelova, D. Saman, P. Slavicek, M. Urbanova, V. Kasicka, F. Teply, *New J. Chem.* **2010**, *34*, 1063–1067; c) A. C. Hernandez-Perez, A. Vlassova, S. K. Collins, *Org. Lett.* **2012**, *14*, 2988–2991; d) J. Vávra, L. Severa, I. Císařová, B. Klepetářová, D. Šaman, D. Koval, V. Kašička, F. Teplý, *Eur. J. Org. Chem.* **2012**, 489–499; e) K. Yavari, S. Moussa, B. Ben Hassine, P. Retailleau, A. Voituriez, A. Marinetti, *Angew. Chem.* **2012**, *124*, 6852–6856; f) L. Severa, M. Ončák, D. Koval, R. Pohl, D. Šaman, I. Císařová, P. E. Reyes-Gutiérrez, P. Sázelová, V. Kašička, F. Teplý, P. Slavíček, *Angew. Chem.* **2012**, *124*, 12138–12142; g) J. Žádný, A. Jančařík, A. Andronova, M. Šámal, J. Vacek Chocholoušová, J. Vacek, R. Pohl, D. Šaman, I. Císařová, I. G. Stará, I. Starý, *Angew. Chem.* **2012**, *124*, 5959–5963; *Angew. Chem. Int. Ed.* **2012**, *51*, 5857–5861.

[3] a) J. Elm, J. Lykkebo, T. J. Sørensen, B. W. Laursen, K. V. Mikkelsen, *J. Phys. Chem. A* **2011**, *115*, 12025–12033; b) A. Latorre, A. Urbano, M. C. Carreno, *Chem. Commun.* **2011**, *47*, 8103–8105; c) M. C. Carreño, Á. Enríquez, S. García-Cerrada, M. J. Sanz-Cuesta, A. Urbano, F. Maseras, A. Nonell-Canals, *Chem. Eur. J.* **2008**, *14*, 603–620.

[4] a) J. E. Field, T. J. Hill, D. Venkataraman, *J. Org. Chem.* **2003**, *68*, 6071–6078; b) J. E. Field, G. Müller, J. P. Riehl, D. Venkataraman, *J. Am. Chem. Soc.* **2003**, *125*, 11808–11809; c) R. Hassey, E. J. Swain, N. I. Hammer, D. Venkataraman, M. D. Barnes, *Science* **2006**, *314*, 1437–1439; d) R. Hassey, K. D. McCarthy, E. S. D. Basak, D. Venkataraman, M. D. Barnes, *Chirality* **2008**, *20*, 1039–1046.

[5] O. Kel, P. Sherin, N. Mehanna, B. Laleu, J. Lacour, E. Vauthey, *Photochem. Photobiol. Sci.* **2012**, *11*, 623–631.

[6] P. Mobian, N. Banerji, G. Bernardinelli, J. Lacour, *Org. Biomol. Chem.* **2006**, *4*, 224–231.

[7] a) J. Guin, C. Besnard, P. Pattison, J. Lacour, *Chem. Sci.* **2011**, *2*, 425; b) D. Conreaux, N. Mehanna, C. Herse, J. Lacour, *J. Org. Chem.* **2011**, *76*, 2716–2722; c) B. Laleu, M. S. Machado, J. Lacour, *Chem. Commun.* **2006**, *0*, 2786–2788; d) A. Ueda, H. Wasa, S. Suzuki, K. Okada, K. Sato, T. Takui, Y. Morita, *Angew. Chem.* **2012**, *124*, 6795–6799; *Angew. Chem. Int. Ed.* **2012**, *51*, 6691–6695; e) C. Nicolas, G. Bernardinelli, J. Lacour, *J. Phys. Org. Chem.* **2010**, *23*, 1049–1056.

[8] T. J. Sørensen, M. F. Nielsen, B. W. Laursen, *ChemPlusChem* DOI: 10.1002/cplu.201402058.

[9] a) J. Guin, C. Besnard, J. Lacour, *Org. Lett.* **2010**, *12*, 1748–1751; b) T. J. Sørensen, A. Ø. Madsen, B. W. Laursen, *Tetrahedron Lett.* **2013**, *54*, 587–590; c) B. Laleu, P. Mobian, C. Herse, B. W. Laursen, G. Hopfgartner, G. Bernardinelli, M. Lacour, *Angew. Chem.* **2005**, *117*, 1913–1917; *Angew. Chem. Int. Ed.* **2005**, *44*, 1879–1883; d) C. Herse, D. Bas, F. C. Krebs, T. Burgi, J. Weber, T. Wesolowski, B. W. Laursen, J. Lacour, *Angew. Chem.* **2003**, *115*, 3270–3274; *Angew. Chem. Int. Ed.* **2003**, *42*, 3162–3166.

[10] F. Torricelli, J. Bosson, C. Besnard, M. Chekini, T. Burgi, J. Lacour, *Angew. Chem.* **2013**, *125*, 1840–1844; *Angew. Chem. Int. Ed.* **2013**, *52*, 1796–1800.

[11] a) B. W. Laursen, T. J. Sørensen, *J. Org. Chem.* **2009**, *74*, 3183–3185; b) B. W. Laursen, F. C. Krebs, *Chem. Eur. J.* **2001**, *7*, 1773–1783; c) B. W. Laursen, F. C. Krebs, *Angew. Chem.* **2000**, *112*, 3574–3576; *Angew. Chem. Int. Ed.* **2000**, *39*, 3432–3434.

[12] For systematic names, see the Supporting Information.

[13] a) J. Griffiths, *Colour and Constitution of Organic Molecules*, Academic Press, **1976**; b) H. Zollinger, *Color Chemistry*, 3rd ed., Wiley VCH, New York, **2001**.
[14] J. C. Martin, R. G. Smith, *J. Am. Chem. Soc.* **1964**, *86*, 2252 – 2256.
[15] R. P. Haugland, *Handbook of Fluorescent Probes and Research Chemicals*, 6th ed., Molecular Probes, Eugene, Oregon, **1996**.
[16] a) P. Hammershøj, T. J. Sørensen, B.-H. Han, B. W. Laursen, *J. Org. Chem.* **2012**, *77*, 5606 – 5612; b) T. J. Sørensen, B. W. Laursen, R. Luchowski, T. Shtoyko, I. Akopova, Z. Gryczynski, I. Gryczynski, *Chem. Phys. Lett.* **2009**, *476*, 46 – 50; c) S. Dileesh, K. R. Gopidas, *J. Photochem. Photophys. A-Chem.* **2004**, *162*, 115 – 120; d) S. Dileesh, K. R. Gopidas, *Chem. Phys. Lett.* **2000**, *330*, 397 – 402; e) E. Thyrhaug, T. J. Sørensen, I. Gryczynski, Z. Gryczynski, B. W. Laursen, *J. Phys. Chem. A* **2013**, *117*, 2160 – 2168; f) T. J. Sørensen, C. B. Hildebrandt, M. Glyvradal, B. W. Laursen, *Dyes Pigm.* **2013**, *98*, 297 – 303; g) T. J. Sørensen, C. B. Hildebrandt, J. Elm, J. W. Andreasen, A. O. Madsen, F. Westerlund, B. W. Laursen, *J. Mater. Chem.* **2012**, *22*, 4797 – 4805; h) B. P. Maliwal, R. Fudala, S. Raut, R. Kokate, T. J. Sørensen, B. W. Laursen, Z. Gryczynski, I. Gryczynski, *PLoS ONE* **2013**, *8*, e63043; i) R. M. Rich, D. L. Stankowska, B. P. Maliwal, T. J. Sørensen, B. W. Laursen, R. R. Krishnamoorthy, Z. Gryczynski, J. Borejdo, I. Gryczynski, R. Fudala, *Anal. Bioanal. Chem.* **2013**, *405*, 2065 – 2075; j) T. J. Sørensen, E. Thyrhaug, M. Szabelski, R. Luchowski, I. Gryczynski, Z. Gryczynski, B. W. Laursen, *Methods and Applications in Fluorescence* **2013**, *1*, 025001.
[17] B. W. Laursen, Ph. D. Thesis, Risø National Laboratory, **2001**.
[18] a) G. A. Olah, *J. Am. Chem. Soc.* **1972**, *94*, 808 – 820; b) G. A. Olah, *Angew. Chem.* **1995**, *107*, 1519 – 1532; *Angew. Chem. Int. Ed.* **1995**, *34*, 1393 – 1405; c) H. H. Freeman, *Carbonium Ions Vol. IV* (Eds.: G. A. Olah, P. v. R. Schleyer), Wiley-Interscience, New York, **1973**.
[19] a) C. Nicolas, J. Lacour, *Org. Lett.* **2006**, *8*, 4343 – 4346; b) K. Maruoka, T. Ooi, *Chem. Rev.* **2003**, *103*, 3013 – 3028.
[20] A. M. Brouwer, *Pure Appl. Chem.* **2011**, *83*, 2213 – 2228.
[21] S. J. Strickler, R. A. Berg, *J. Chem. Phys.* **1962**, *37*, 814.
[22] COLLECT Software, Nonius BV, **1997 – 2001**.
[23] Sheldrick, G. M. (2008), Acta Crystallogr. A64, 112 – 112.
[24] P. Mobian, C. Nicolas, E. Francotte, T. Bürgi, J. Lacour, *J. Am. Chem. Soc.* **2008**, *130*, 6507 – 6514.

Received: January 8, 2014
Published online on April 15, 2014